15th Triennial World Congress, Barcelona, Spain

# INTELLIGENT OPTIMIZATION CONTROL FOR LAMINAR COOLING[1]

**CHAI Tianyou[*], TAN Minghao[*], CHEN Xiaoyan[*], LI Hanxiong[**]**

[*] *Research Centre of Automation, Northeastern University, China, 110004*
[**] *Department of Manufacturing Engineering and Engineering Management, City University, Hong Kong*

**Abstract:** The laminar cooling of hot slabs is a distributed-parameter system characterized by time varying, nonlinear factors and physical difficulties in continuous temperature measurement. The process operation is classified into operating points according to steel No., thickness and target temperature. The moving slab is divided into segments upon which the control is to be implemented. The technology of soft sensing is incorporated into the temperature prediction model of the process that is adapted online to find the temperature profile through thickness, which will be used for online error correction in closed-loop control. Industrial experiments have shown the effectiveness of the proposed method. *Copyright © 2002 IFAC*

Keywords: laminar cooling control, distributed control, optimization, modeling, soft sensing, supervisory control.

## 1. INTRODUCTION

The laminar cooling of hot slabs is a key process in hot rolling that not only shortens the cooling time of the slab but also improves the quality of the finished product (Groch, *et al*., 1990). The process represents a typical distributed parameter system described by partial differential equations with the thermal field of the slab varying in terms of both time and position (James, *et al*., 1993). Furthermore, the heat transfer mechanism of the process is complicated by time varying and strong nonlinear factors as well (Dietmar, *et al.,* 1998)

The cooling process is traditionally controlled by DCS. The complex process requires human supervision on site to optimize the control operation from time to time by adjusting the control set points (Cui, 2001).

However, this makes the quality control of the process affected by unreliable human factors. Since many information of the cooling process can not be measured online, it is very difficult to apply conventional feedback control on the supervision level (Guan, *et al.,* 1997). It is noted that most existing control methods only apply to thinner slabs and the performance quickly deteriorates when the slab becomes thicker, which causes economic losses to manufacturers (Guan, *et al* 1997).

Because the slab temperature can not be measured continuously, a physical model of the cooling process is set up using the technique of soft sensing and finite discretization to predict the through-thickness and lengthwise temperature distribution in the entire cooling process (Van, 1993) and for feedback control. In addition, nonlinear control and adaptive control techniques are combined in this paper to form an intelligent optimization control framework for the laminar cooling system.

[1] This work was supported by the Chinese National Natural Science Foundation No. 60074116.

## 2. PROCESS ANALYSIS AND MODELING

### *2.1 Process description*

The general layout for the laminar cooling process is shown in Fig.1 with top headers and bottom sprays. After leaving the finishing mill, the slab is cooled with water on the runout table in the cooling zone extending from EMP to HMP. EMP is the entry point to the cooling zone where temperature and thickness of the slab are measured. HMP is the point where the temperature of the slab is measured before being coiled at the downcoiler.

The whole cooling process can be classified into air-cooling, which is uncontrollable, and water-cooling, which is further divided into the main cooling zone and the fine cooling zone separated by FBP. Nineteen banks of four headers are installed on the runout table, with each header as one cooling unit controlled by a valve. Each header has a fixed flow rate and only the number of active headers or cooling length can be manipulated. The functional model of the process is shown in Fig.2 .

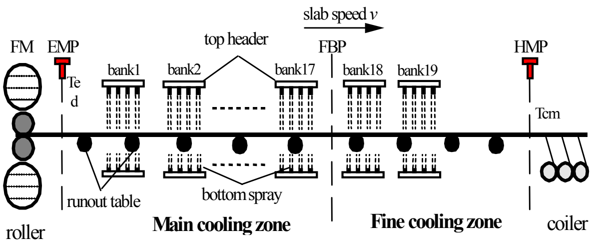


Fig. 1. Layout of the laminar cooling process on the runout table.

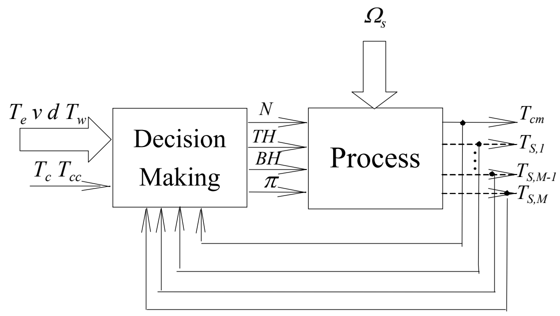


Fig.2 Functional model of the cooling process

*Where: TH—top start header, BH—bottom start header, d —thickness of slab, v—runout table speed, $T_e$—entry temperature, $T_c$—target coiling temperature, $T_{cc}$—cooling curve, $T_w$—water temperature, N—active headers, π—spraying pattern, $T_{cm}$—coiling temperature measurement, $\Omega_s$—disturbances ($T_{env}$ , w, l and a). l—length of slab, w—width of slab, a— runout table acceleration, $T_{env}$— environment temperature.*

The laminar cooling process is a complex system influenced by many factors including the thickness and shape of the slab, runout table velocity, environment and water temperature. The objective of laminar cooling is to maintain the desired temperature throughout the slab and achieve a constant cooling rate to ensure consistent physical properties within the slab.

The control is implemented by switching on or off the sprays in the cooling process and adjusting the number and distributions of the water sprays. The cooling rate is controlled through use of different spraying patterns for the headers. There are 4 major spraying patterns of water cooling as shown in table 1.

Table 1 Spraying configuration.

| Spraying pattern | Header configuration | |
|---|---|---|
| A | intensive pattern | 1111 |
| B | 3/4 staggered pattern | 1110 |
| C | 2/4 staggered pattern | 1010 |
| D | 1/4 staggered pattern | 1000 |

Note: "1" indicates header is open,"0" indicates closed.

### *2.2 Modeling*

The complexity of the cooling process makes the temperature distribution of the slab depend on both time and location, and the physical parameters of the slab vary with temperature. For a good performance, each slab has to be classified into segments. Each segment is controlled to have the same desired temperature throughout its thickness.

Heat conduction dynamics at each segment, for example the k[th] segment, of the slab during the cooling process is described by the following partial differential equation (Guan, *et al.*, 1997):

$$\frac{\partial T_k(y,t(k))}{\partial t(k)} = a\frac{\partial^2 T_k(y,t(k))}{\partial y^2} \tag{1}$$

with the initial condition:

$$T_k(y,t(k)) = T_k^0(y) \tag{1a}$$

and boundary conditions:

$$\begin{cases} \lambda \left.\dfrac{\partial T_k(y,t(k))}{\partial y}\right|_{y=\frac{h}{2}} = \alpha_{k,0}[T_{w0}(x_{k0} + \int_{t_{k0}}^{t(k)} v(t)dt, t) - T(0,t(k))] \\ \lambda \left.\dfrac{\partial T_k(y,t(k))}{\partial y}\right|_{y=-\frac{h}{2}} = \alpha_{k,M}[T_{wM}(x_{k0} + \int_{t_{k0}}^{t(k)} v(t)dt, t) - T(h,t(k))] \\ \left.\dfrac{\partial T}{\partial y}\right|_{y=0} = 0 \end{cases} \tag{1b}$$

where $a$: the thermal diffusivity of the slab; $\lambda$: thermal conductivity of the slab; $\alpha_{k,i}$: heat transfer coefficient of segment $k$; $T_{wi}$: coolant temperature *(i=0- top surface; i=M- bottom surface)*; $h$: thickness of segment $k$; $x_k$: lengthwise coordinate of segment $k$ at time $t_{k0}$; $T_k(y,t(k))$: the through-thickness temperatures of segment $k$ at time $t(k)$.

Through finite discretization the above equations can be implemented. A three-dimensional dynamic equation is developed in (2) to take into account both the through-thickness and lengthwise temperature distribution over time. Thus, the through-thickness temperatures can be predicted for any point in the slab at any time and at any specified location along the runout table (Guan, *et al*., 1997).

$$\begin{cases}(1+f_0+f_0\beta_0)T_0(n+1)-f_0T_1(n+1)= \\ (1-f_0-f_0\beta_0)T_0(n)+f_0T_1(n)+2f_0\beta_0T_{w,i} \\ (2+2f_j)T_j(n+1)-f_jT_{j-1}(n+1)-f_jT_{j+1}(n+1)= \\ f_jT_{j-1}(n)+(2-2f_j)T_j(n)+f_jT_{j+1}(n)\ \ (j=1,2\cdots M-1) \\ (1+f_M+f_M\beta_M)T_M(n+1)-f_MT_{M-1}(n+1)= \\ f_MT_{M-1}(n)+(1-f_M-f_M\beta_M)T_M(n)+2f_M\beta_MT_{w,i}\end{cases} \quad (2)$$

where $j$: thickness node; $n$: time node; $\Delta\Gamma$: time step size; $\Delta y$: thickness step; $T_{w,i}$: water coolant temperature; $T_j(n)$: temperature of thickness node $j$ during the cooling time at $n^{th}$ time step; $f_j$ (Fourier number) $= a_j\frac{\Delta\Gamma}{(\Delta y)^2}$; $\beta_i$ (Biot number) $=\frac{\alpha_i.\Delta y}{\lambda_i}$; $a_j$: thermal diffusivity of the slab at node $j$; $\alpha_i$: heat transfer coefficient; $\lambda_i$: thermal conductivity.

The discussion of the various parameters in the physical model (2) is given below:

*Heat transfer coefficient.* The heat transfer coefficient for water-cooling has to do with runout table velocity, slab thickness, surface temperature of the slab, water temperature, water flow rate and random factors. In addition, the significant heat evolved during the phase transformation from austenitic (γ-Fe) to ferritic (α-Fe) due to the water cooling also has a dramatic impact on the heat transfer coefficient but can not be quantified. Since air-cooling is uncontrollable, only water cooling is considered for direct control in this paper.

A common approach to modelling the heat transfer coefficient is to use various functions whose parameters are to be determined through practical identification experiments. After the analysis of large amounts of data, an empirical expression is developed of the heat transfer coefficient as the function of the speed of the runout table, thickness of the slab and surface temperature of the slab:

$$\alpha_i = k\left(\frac{v_i}{v_{op,i}}\right)^{\gamma_1}\left(\frac{d_i}{d_{op,i}}\right)^{\gamma_2}\left(\frac{Te_i}{Te_{op,i}}\right)^{\gamma_3} \quad (3)$$

where $v_i$, $d_i$ and $Te_i$ are speed of the runout table, thickness and surface temperature of the slab segment at the specified cooling unit respectively; $v_{op,i}$, $d_{op,i}$ and $Te_{op,i}$ are speed of the runout table, thickness and surface temperature of the slab segment at workpoints respectively. $k$, $\gamma_1$, $\gamma_2$ and $\gamma_3$ are values that define the effect of runout table speed, segment thickness and segment surface temperature on the heat transfer coefficient. An initial estimate of $k$, $\gamma_1$, $\gamma_2$ and $\gamma_3$ are performed offline and they are adapted online.

*Thermal diffusivity.* Thermal diffusivity is related to slab material and temperature and is represented by the empirical curve as shown in Fig.3.

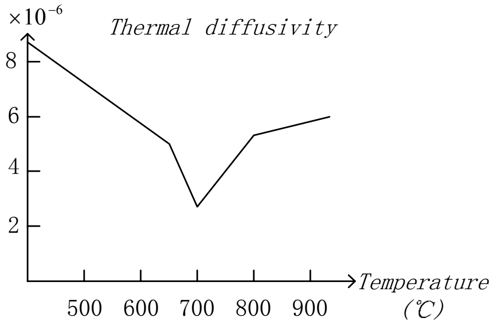


Fig.3 Thermal diffusivity curve

*Thermal conductivity.* Thermal conductivity is connected to the material and temperature of the slab and changes during the cooling process. Researches have shown that it is linearly related to the temperature of the slab to some extent. Based on the analysis of large amounts of real time data collected from the process it has been found that the speed of the slab has a major influence on the cooling process. This influence is integrated into thermal conductivity in the following form:

$$\lambda_i = 56.43-\left(\frac{41.91-25.57}{850.0-400.0}+c_i(v_i-v_{op,i})\right)\times T_i \quad (4)$$

where $c_i$, either a constant or a function, is the speed coefficient, $v_{op,i}$ is the base speed, $T_i$ is temperature of the slab segment under the current cooling unit (Celsius) and $c_i$ and $v_{op,i}$ are related to the grade, thickness and speed of the slab segment.

## 3. CONTROL METHODOLOGY

Due to the uncontrollable dynamics and other boundary variations as depicted in Fig.2, the cooling performance is not very satisfactory. Closed-loop feedback control at the supervision level is one feasible solution to optimize the cooling performance without human intervention. However, it is impossible to measure the coiling temperature online during the laminar cooling. Without measurement, it is impossible to do feedback control. To overcome this problem, the temperature prediction error is used in online adaptation to provide closed-loop control.

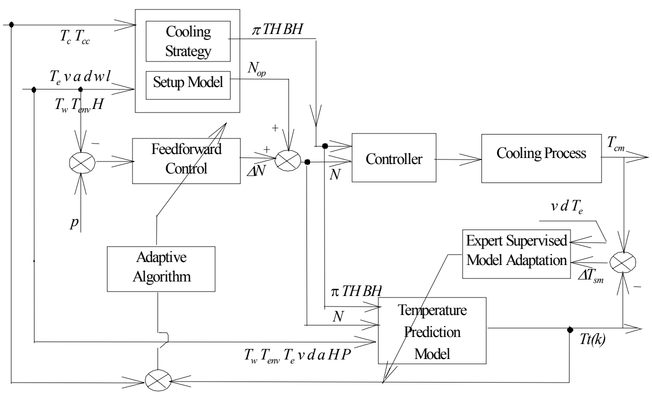


Fig. 4 Framework for the intelligent optimization of cooling control

*p—workpoint values; $T_c$—target coiling temperature (℃); H—slab grade; π—spraying pattern; Tt(k)—model predicted temperature of segment k;*

The process can be linearized around the nominal operating points to simplify the dynamic optimization. The real operating point is thus composed of the nominal operating point plus an adaptation around that point. Based on this idea, the control methodology can be developed as shown in Fig.4 to have two major mechanisms for setpoint optimization. The setup model is to provide a nominal operating point for DCS or controllers at the lower level; while feedforward control is to provide the required adaptation around the nominal point to compensate for the influence from the uncontrollable dynamics and boundary variations.

Because of the time-varying temperature distribution along both the length and thickness of the slab, it is sampled into segments at a fixed time interval, or control cycle. The slab is "caught" the instant it threads EMP and from that moment on it is tracked all the way to the downcoiler with respect to its speed and position.

*Intelligent optimisation*. The system is capable of self-learning which includes adaptive algorithm for feedforward control and model learning. The self-learning happens at inter-segment level within the same slab and inter-slab level according to steel grade, size and cooling strategy. A long-term learning for certain material categories is also performed. Each time a segment head reaches the pyrometer at HMP, the real cooling run of that segment is used to compare model output with reality.

*Cooling strategy.* Because there is only one process model in (2), it is impossible to determine the number of active headers $N$ without knowledge of other parameters. The top and bottom start headers are determined by the cooling strategy, as well as the spraying pattern $\pi$. The cooling strategy provides a precalculation through consideration of some boundary conditions for process model (2), after which the nominal number of headers $N_{op}$ can be found through recursive calculation of the process model (2).

$T_{cc}$ gives the cooling curve from which the critical temperature can be obtained. Once the temperature of the slab is reduced to the critical temperature, the cooling rate can not exceed certain limits, otherwise the slab risk quality deformation due to the physical transitions in the steel. For this reason, the staggered spraying pattern is used after the critical temperature is reached.

*Setup model.* The setup model is classified into different parts for different control variables. Boundary variations of slabs on entering the cooling section, which is mathematically unmodelled, will upset the cooling performance. In reality the operating points are determined through slab classifications according to grade, thickness and required target temperature.

*Feedforward control* (Guo, 1997). The required header number correction for the slab segment currently under the entry pyrometer is calculated by feedforward control. Any change in the number of sprays is scheduled to occur when the affected slab segment reaches the appropriate spray unit along the runout table. A heuristic model below is used to calculates the dynamic correction for the number of water sprays.

$$\Delta N = N_{op}(\eta_1 \frac{Te - Te_{op}}{Te_{op}} + \eta_2 \frac{v - v_{op}}{v_{op}} + \eta_3 \frac{d - d_{op}}{d_{op}} + \eta_4 \frac{T_w - T_{w,op}}{T_{w,op}}) \quad (5)$$

where: $N_{op}$ is the nominal number of headers; the first term in the bracket allows for the compensation of entry temperature variation; the second term for the compensation of speed variation; the third for slab thickness variation and the fourth for water temperature variation. $\eta_1$, $\eta_2$, $\eta_3$, $\eta_4$ are adaptation coefficients for compensation of the deviations of entry conditions from workpoint conditions.

In case of changing process dynamics due to process noise or modelling error, the heuristic model (5) on which the feedforward control is based should be updated. In light of this the four parameters ($\eta_1$, ..., $\eta_4$) in (5) are adapted online. This requires other modeling and control techniques as described below.

*Adaptive algorithm for feedforward control.* The heuristic model (5) is updated using the difference between the target temperature and the model prediction. Recursive LS algorithm with forgetting factors is used as follows in the identification:

$$y = \varphi^T \theta \quad (6)$$

where

$$y = \Delta N \quad (6a)$$

$$\varphi^T = [\frac{Te - Te_{op}}{Te_{op}} N_{op}, \frac{v - v_{op}}{v_{op}} N_{op}, \frac{d - d_{op}}{d_{op}} N_{op}, \frac{T_w - T_{w,op}}{T_{w,op}} N_{op}] \quad (6b)$$

$$\theta^T = [\theta_1, \theta_2, \theta_3, \theta_4] \quad (6c)$$

$$\hat{\theta}(J+1) = \hat{\theta}(J) + K(J)[y(J+1) - \varphi^T \hat{\theta}(J)] \quad (7a)$$

$$K(J) = P(J)\varphi[\lambda_f + \varphi^T P(J)\varphi]^{-1} \quad (7b)$$

$$P(J+1) = \frac{1}{\lambda_f}[P(J) - P(J)\varphi(\lambda_f + \varphi^T P(J)\varphi)^{-1}\varphi^T P(J)] \quad (7c)$$

where $\lambda_f$ is the forgetting factor, $0 \le \lambda_f \le 1$.

In order to perform the recursive identification in (6) $\Delta N$ must be found. This is done through an expert system which based on expert experience obtains $\Delta N$ from the difference between the target and the predicted coiling temperature.

*Model learning.* Because the heat transfer coefficient for water cooling has the most influence on the model accuracy, temperature prediction error of the process is corrected by means of the online adaptation of $\alpha$. The model learning consists of the expert supervised adaptation of the heat transfer coefficient $\alpha$. The coefficients $k$, $\gamma_1$, $\gamma_2$, $\gamma_3$ in (3) are recursively identified based on soft measurements and process experience also using the algorithm in (7).

Fuzzy reasoning is used to find $\alpha$ since it is needed for the recursive identification in (7). Due to the lack of information about the moving slab between the entry and exit of the cooling zone during cooling, the difference between the real coiling temperature and the model prediction by (2) is fed to an expert system to give the variation of $\alpha$.

The input variables for the expert reasoning are slab velocity, slab thickness, slab temperature and the temperature prediction error, i.e. $T_{cm}-Tt(k)$. They are labeled $X_1$, $X_2$, $X_3$ and $X_4$ respectively. The output variable is the variation of $\alpha$, which is labelled Y. The membership functions are shown in Fig. 5 and Fig. 6.

The fuzzy rules are classified according to steel No., thickness and the coiling temperature. The reasoning process of this system sheds some light on the real working mechanism of the real time process. For example, if the actual coiling temperature is higher than the target coiling temperature it is obvious that the control system assumed an $\alpha$ greater than the actual one. So there should be a reduction in $\alpha$. The reverse is true if the actual coiling temperature is lower than the target coiling temperature.

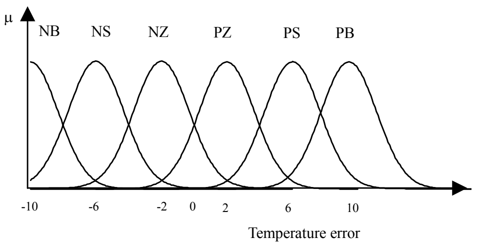


Fig.5. Input Membership functions

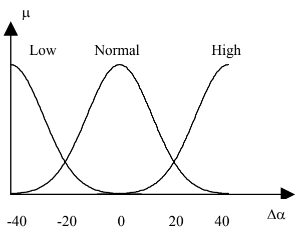


Fig.6. Output Membership functions

The expert system finds $\Delta\alpha$ *(i=1,2,3)* based on the following rules.

if $X_1$ is $A_{11}$ and $X_2$ is $A_{12}$ and … and $X_4$ is $A_{14}$ then Y is $B_1$ else
if $X_1$ is $A_{21}$ and $X_2$ is $A_{22}$ and … and $X_4$ is $A_{24}$ then Y is $B_2$ else
… …
if $X_1$ is $A_{m1}$ and $X_2$ is $A_{m2}$ and … and $X_4$ is $A_{m4}$ then Y is $B_m$

where m=6. It represents a fuzzy relationship on $X_1 \times X_2 \times ... \times X_4 \times Y$ :

$$\tilde{R}_i(\tilde{A}_{i1}, \tilde{A}_{i2}, ..., \tilde{A}_{i4}; \tilde{B}_i) \qquad i = 1,2,...,m \qquad (10)$$

After the expert reasoning, the output Y is defuzzified to obtain $\Delta\alpha$, which is added to the workpoint value to result in $\alpha$. In this way, the heat transfer coefficient $\alpha_i$ is adapted.

## 4. SIMULATIONS AND INDUSTRIAL EXPERIMENTS

### *4.1 Simulations*

Table 2 Experiment conditions

| Setpoint | Boundary Conditions | | | |
|---|---|---|---|---|
| $T_c$ | $v$ | $Te$ | $d$ | $T_w$ |
| 600 | 3.14 | 846 | 11.14 | 29 |
| $N$ | $\pi$ | $TH$ | $BH$ | |
| 37 | **A** | 17 | 99 | |

As shown below, the entry temperature has a fluctuation of around 30℃. By using the proposed control method, the cooling temperature remains within 5 ℃ of the target temperature, which demonstrates the effectiveness of the method.

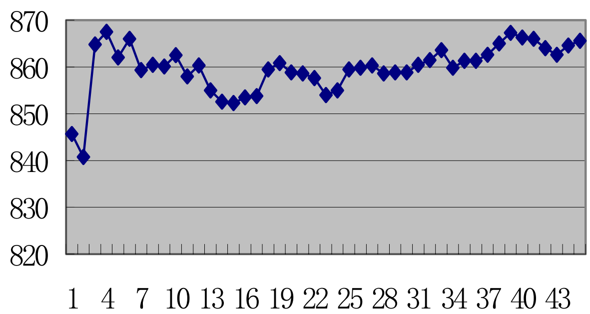


Fig.7a. Entry temperature profile

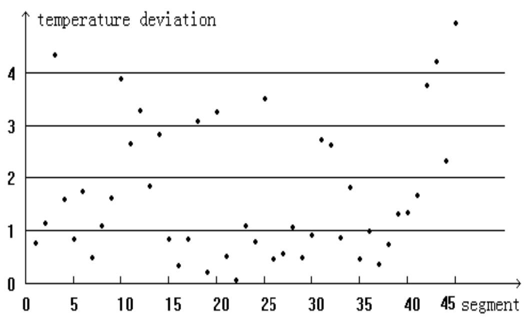


Fig.7b. Coiling temperature deviation

### *4.2 Industrial Experiments*

Table 3 Experiment conditions

| Setpoint | Boundary Conditions | | | |
|---|---|---|---|---|
| $T_c$ | $V$ | $Te$ | $d$ | $T_w$ |

| | | | | |
|---|---|---|---|---|
| *600* | *3.04* | 844 | 11.14 | 29 |

| Control Variables | | | |
|---|---|---|---|
| *N* | $\pi$ | *TH* | *BH* |
| 31 | **A** | 17 | 99 |

*Experiment results.* The results for the industrial experiments are shown in Fig.8.

The entry temperature is shown in Fig.8a which has a variation of nearly 45℃. It can be seen from Fig.8b that the real coiling temperature has a variation of nearly 40℃ without feedforward control and within 10 ℃ with the proposed intelligent optimization control in Fig.8c.

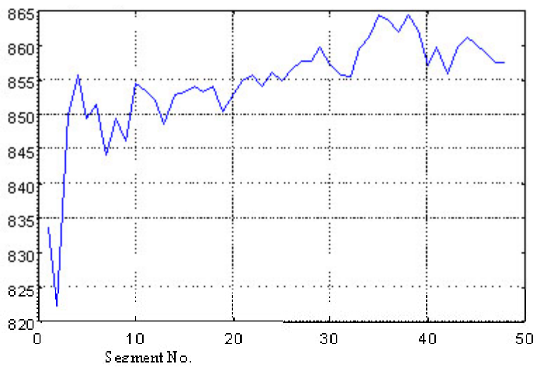


Fig.8a. Entry Temperature

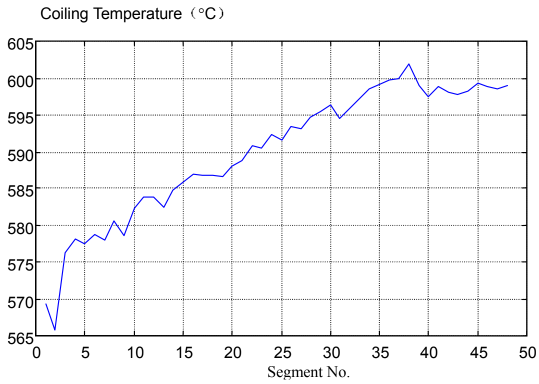


Fig.8b. Without feedforward control

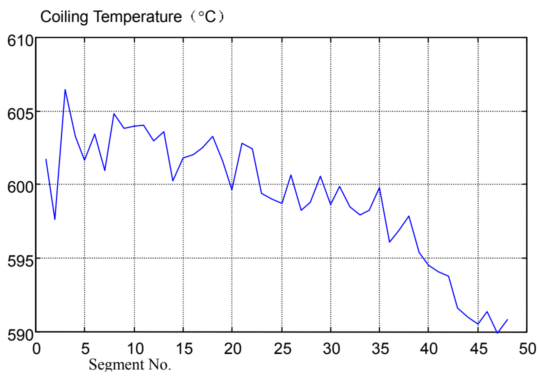


Fig.8c. With intelligent optimization control

## 5. CONCLUSIONS

The laminar cooling process of hot slabs has strong nonlinear and time-varying features, with uncontrollable and immeasurable dynamics.

In this paper, the intelligent control is applied in the supervision loop to optimize the cooling performance. The control provides nominal operating points and their adaptations for DCS at low-level, with respect to segments along the length of the slab, steel No., thickness and the target temperature of the slab. The technology of soft sensing is incorporated into the process model to find the through-thickness temperature distribution, and makes the through-thickness temperature control feasible. The system has models adapted online and is capable of self-learning.

Industrial experiments at a certain steel plant have shown that the proposed method can achieve the desired final cooling temperature with high accuracy, and could be generalized to deal with slabs at gages thicker than 20mm.

## REFERENCES


Auzinger, Dietmar, Franz Parzer and Gerhard Posch (1998). Process optimization for laminar cooling. *Iron and Steel Engineer,* **75**, pp. 45-49.

Cui, Jianjiang, Wu Wenbin, Cai Yi, *et al* (2001). Thickness error prediction for setting roll gap based on neural networks. *Basic Automation,* **8**,**S** pp. 70-72.

Evans, James F., Iain D. Roebuck and Howard R.Walkins (1993). Numerical modeling of hot strip mill runout table cooling. *Iron and steel engineer.* no.1, **70**, pp. 50-55.

Groch, Andrzej G., Robert Gubemat and Emmanuel R. Birstein (1990). Automatic control of laminar flow cooling in continuous and reversing hot strip mills. *Iron and Steel Engineer,* **67**, pp. 16-20.

Guan, Shouping, Xiaobo Wang and Tianyou Chai, Xiaogang Wang (1997). "The slab accelerating cooling system control model and its application". The Proc.of ASI.

Guo,Remn-Min (1997). Modeling and simulation of run-out table cooling control using feedforward-feedback and element tracking system*[J]. IEEE transactions on industry applications,* **33**, pp. 304-311.

Van, Ditzhuijzen G (1993). The controlled cooling of hot rolled strip: a combination of physical modeling, control problems and practical adaptation. *IEEE transactions on automatic control[J],* **38**, pp. 1060-1065.